Article

Cite This: *Biomacromolecules* 2019, 20, 3494−3503

pubs.acs.org/Biomac

Understanding the Coacervate-to-Vesicle Transition of Globular Fusion Proteins to Engineer Protein Vesicle Size and Membrane Heterogeneity

Yeongseon Jang,[†,‡,∥] Ming-Chien Hsieh,[†,§] Dylan Dautel,[†] Sherry Guo,[†] Martha A. Grover,[†] and Julie A. Champion*[,†]

[†]School of Chemical and Biomolecular Engineering, Georgia Institute of Technology, 950 Atlantic Drive NW, Atlanta, Georgia 30332, United States

[‡]Department of Chemical Engineering, University of Florida, 1006 Center Drive, Gainesville, Florida 32611, United States

[§]Department of Chemistry, Emory University, Atlanta, Georgia 30322, United States

Supporting Information

ABSTRACT: Protein-rich coacervates are liquid phases separate from the aqueous bulk phase that are used by nature for compartmentalization and more recently have been exploited by engineers for delivery and formulation applications. They also serve as an intermediate phase in an assembly path to more complex structures, such as vesicles. Recombinant fusion protein complexes made from a globular protein fused with a glutamic acid-rich leucine zipper (globule-Z_E) and an arginine-rich leucine zipper fused with an elastin-like polypeptide (Z_R-ELP) show different phases from soluble, through an intermediate coacervate phase, and finally to vesicles with increasing temperature of the aqueous solution. We investigated the phase transition kinetics of the fusion protein complexes at different temperatures using dynamic light scattering and microscopy, along with mathematical modeling. We controlled coacervate growth by aging the solution at an intermediate temperature that supports coacervation and confirmed that the size of the coacervate droplets dictates the size of vesicles formed upon further heating. With this understanding of the phase transition, we developed strategies to induce heterogeneity in the organization of globular proteins in the vesicle membrane through simple mixing of coacervates containing two different globular fusion proteins prior to the vesicle transition. This study gives fundamental insights and practical strategies for development of globular protein-rich coacervates and vesicles for drug delivery, microreactors, and protocell applications.

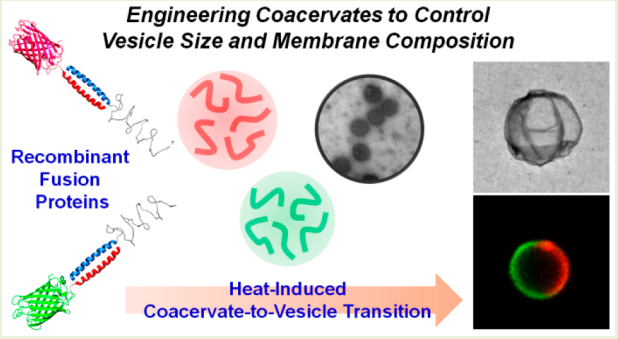

INTRODUCTION

Vesicles are critical structures in many aspects of cellular functions.[1] Inspired by vesicles in living systems, artificial vesicles have been actively developed for both basic studies, such as to understand biophysical processes occurring at cell membranes, and practical applications, including fabrication of microreactors and targeted delivery vehicles.[2,3] The size and membrane properties of synthetic vesicles play a critical role in determining vesicle functionality. For example, sub-μm-scale vesicles with stimuli-responsive membrane components are useful for drug delivery applications,[4] whereas giant unilamellar vesicles made from different phospholipids serve as model systems to mimic the essential features of cell membranes.[5]

To create complex synthetic vesicles, approaches mainly use interfacial assembly of amphiphilic lipids or synthetic diblock copolymers in water-in-oil emulsions.[6,7] For example, multi-compartment lipid vesicles can be created by transferring droplets between an oil and aqueous solution several times.[8] Microfluidics is a powerful tool to create heterogeneous and/or asymmetric vesicle membranes of lipids or polymers through water/oil/water double emulsions.[9,10] Gel-assisted lipid swelling methods are used to make giant vesicles composed of different lipid molecules.[11,12] The pathways to control vesicle structure are diverse and vary by molecular structure, assembly properties, and dynamic behavior of the individual molecular building blocks.

Coacervates, which are spherical liquid droplets separate from the surrounding aqueous liquid phase, can also serve as a transient phase in a more complex assembly path to vesicles and other structures.[13] Formation of dense protein-rich droplets is a natural and essential process for the growth and development of cells.[14] Coacervation of tropoelastin by thermal and osmotic triggers is a typical example that can be found in nature, which induces the assembly of elastin fibers *in*

Received: June 4, 2019
Revised: August 10, 2019
Published: August 28, 2019

DOI: 10.1021/acs.biomac.9b00773
Biomacromolecules 2019, 20, 3494−3503

vivo.[15] Recombinantly engineered elastin-like polypeptides (ELPs) made from the tropoelastin sequence allow the development of biomaterials that mimic the material properties of native elastin while exhibiting lower critical solution temperature (LCST) behavior. ELP-based coacervates have been developed as attractive biomedical platforms for tissue engineering scaffolds and drug delivery vehicles.[16−18]

Since coacervation is induced by electrostatic or hydrophobic forces between building molecules in an aqueous environment, coacervate droplets have the benefit of encapsulating functional globular proteins into higher-ordered, self-assembled materials without the use of organic solvents that can hamper bioactivity.[19] Previous studies have shed light on the coacervate-to-vesicle transition of lipids[20] and polyelectrolyte complexes.[21] For example, Kimato and coauthors demonstrated the simple coacervation of a glycolipid biosurfactant and chemically induced phase transition of coacervates to vesicles.[20] Alternatively, coacervates made from polyelectrolyte complexes transitioned into vesicles under irradiation with a focused infrared laser in an optical tweezer setup.[21] Although these examples provide inspiration to understand the process by which an ordered vesicle membrane is generated from coacervates, the requirement of chemical modification of the molecular components or laser irradiation can be limiting for proteins or other biomolecules.

More recently, liquid−liquid phase separation during self-assembly of amphiphilic block copolymers into vesicles has been observed experimentally by liquid-phase electron microscopy and supported computationally with Gibbs free energy calculations.[22] This work reported that coacervates act as a precursor in the formation of higher-ordered, polymeric assemblies such as micelles and vesicles while playing a role in determining the resulting self-assembled structures.[22] A transition between the liquid−liquid phase separation and the self-assembly into a highly organized structures can be determined by comparing the mixing Gibbs energy density of the two different phases based on Flory−Huggins mean-field lattice theory.[23] With the gradual increase of the molecular amphiphilicity of a diblock copolymer, micellization is preferred over coacervation, and the final assembled-structures are dependent on the building block properties such as degree of polymerization.[24] The understanding of the transition mechanism from molecules to assemblies needs to be expanded toward diverse building molecules, since to our best knowledge there is no example of the coacervate-to-vesicle transition in protein-based building molecules.

Previously, we reported the phase transition of recombinantly engineered ELP fusion proteins from soluble to coacervates to vesicles as a function of temperature and protein concentration.[25] The recombinant ELP fusion protein, an arginine-rich cationic leucine zipper fused to an ELP domain (Z_R-ELP), forms a strong complex with a globular mCherry protein fused to a glutamic acid-rich leucine zipper (mCherry-Z_E) via high affinity binding of the leucine zippers.[26,27] The globule-zipper-ELP complexes serve as amphiphilic building blocks to form vesicles upon heating above the temperature range of the ELP phase transition (defined as the T_t range). We also observed that the recombinant proteins start to associate into coacervate droplets at temperatures low in the T_t range before the transition into the organized vesicle structure upon further warming.[25] This observation motivated the current study on the phase transition of globule-zipper-ELP fusion proteins upon heating to reveal scientific and engineering insights to understand the transition pathway and to control the final self-assembled vesicle size and structure.

Here, we employ globule-Z_E (i.e., mCherry-Z_E and enhanced green fluorescent protein (eGFP)-Z_E) and Z_R-ELP proteins to investigate the kinetics of their phase transition by monitoring formation and growth rates of coacervates and vesicles. The changes in solution turbidity and size and morphology of coacervates and vesicles are investigated by light absorbance, dynamic light scattering, and microscopy as a function of incubation time at different temperatures. Also, we develop a mathematical model of a two-step self-assembly process to support the mechanisms of coacervation and vesicle formation as a function of protein solubility, which strongly depends on temperature. The results reveal a strategy for controlling vesicle size and membrane composition heterogeneity by tuning coacervate properties via time, temperature, and mixing.

EXPERIMENTAL SECTION

Expression and Purification of Recombinant Fusion Proteins. This work used three recombinant fusion proteins, Z_R-ELP, an arginine-rich basic leucine zipper (Z_R) fused with a thermoresponsive elastin-like polypeptide (ELP), and globule-Z_E proteins, a globular domain, either mCherry or enhanced Green Fluorescent Protein (eGFP) fused with a glutamic acid-rich leucine zipper (Z_E). The ELP sequence $[(VPGVG)_2(VPGFG)(VPGVG)_2]_5$ was used in this study. Plasmid construction, transformation, and protein expression and purification steps are described in detail in our previous reports.[25,28] Briefly, *E. coli* (BL21) containing pQE60 plasmids either pQE60-His6-Z_E/Z_R-ELP, pQE60-mCherry-Z_E-His6, or pQE60-eGFP-Z_E-His6 were grown separately at 37 °C in Lysogeny broth (LB) media (10 g casein, 5 g yeast extract, and 10 g NaCl) with antibiotics (200 mg/L ampicillin, 34 mg/mL chloramphenicol). Isopropyl-β-thiogalactoside (IPTG, 1.0 mM) was added when the solution optical density at 600 nm (OD_{600}) reached 0.8. After 5 h of IPTG induction, cells were harvested by centrifugation and resuspended in lysis buffer. The lysis, wash, and elution procedures for protein purification were conducted according to manufacturer instructions (Qiagen). The Z_R-ELP was purified in denaturing conditions using 8 M urea buffers, eluted with 6 M guadinine hydrochloride, then dialyzed into deionized water. The functionally folded, globular domain-fused mCherry-Z_E and eGFP-Z_E proteins were purified in native conditions using imidazole buffers, then dialyzed into phosphate buffered saline (PBS, pH 7.4). The size and purity of the purified proteins were analyzed by sodium dodecyl sulfate polyacrylamide gel electrophoresis (SDS-PAGE) following boiling in gel loading buffer containing reducing agent (Figure S1 of the Supporting Information, SI).

Monitoring of Vesicle Formation Kinetics and Transition Temperature. The fusion proteins, 30 μM of Z_R-ELP and 1.5 μM of mCherry-Z_E, were mixed in PBS containing 0.3 M NaCl on ice for 15 min. To characterize vesicle formation kinetics, 100 μL of the protein mixture solution was placed in a microplate reader (Synergy H4 Hybrid Multi-Mode Microplate Reader, BioTek Instrument), and incubated at 25 °C while reading turbidity changes of the solution (optical density at 400 nm). Also, morphological changes of structures in the protein mixture solution at room temperature were recorded by a fluorescent microscope (Axio Observer, Carl Zeiss) for 1 h. The turbidity changes of the samples upon coacervation were monitored by a spectrometer (Chirascan-plus CD, Applied Photophysics) while increasing the temperature from 5 to 50 °C with a heating rate of 1 °C/min to determine the transition temperature range (T_t range) of the soluble proteins. Turbidity changes upon cooling from 50 to 5 °C with a cooling rate of 1 or 0.1 °C/min.

Characterization of Coacervates and Vesicles Self-Assembled in the Protein Mixture Solutions. Hydrodynamic diameter (D_H (nm)) of self-assembled structures in the protein mixture solutions of mCherry-Z_E and Z_R-ELP was measured by

DOI: 10.1021/acs.biomac.9b00773
Biomacromolecules 2019, 20, 3494−3503

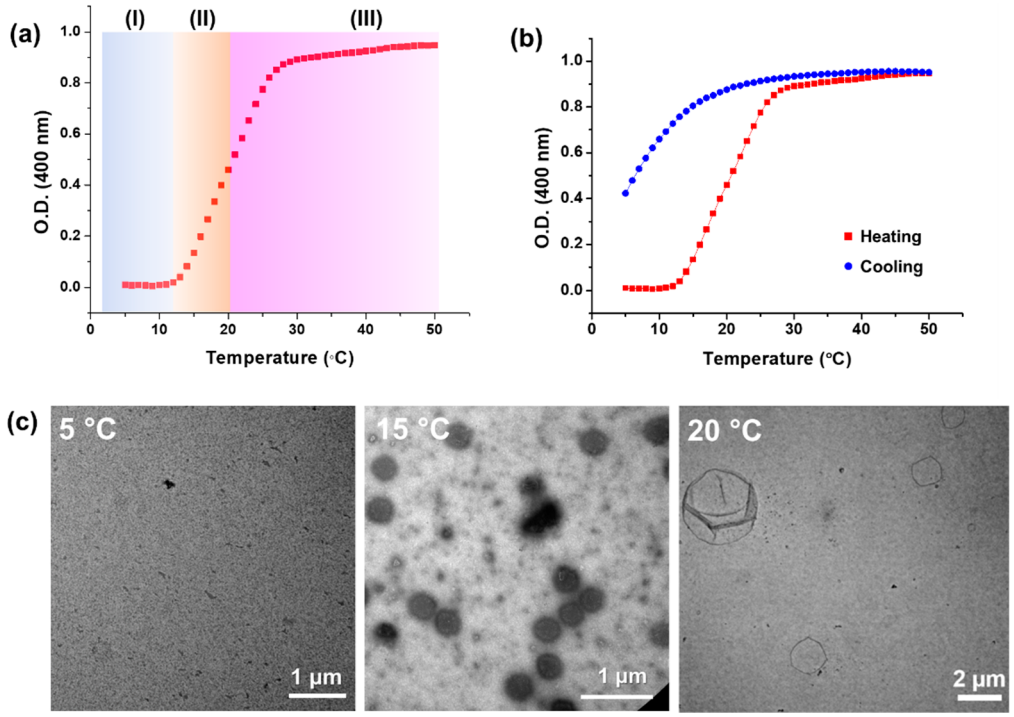

Figure 1. (a) The turbidity changes and (b) thermal hysteresis of heating and cooling profiles of a fusion protein mixture solution containing mCherry-Z_E and Z_R-ELP, obtained by measuring the optical density at 400 nm with heating and cooling rates of 1 °C/min. (c) TEM images of samples at 5, 15, and 20 °C.

dynamic light scattering (DLS) (Zetasizer NanoZS, Malvern Instruments). A 4 mW He−Ne laser operating at a wavelength of 633 nm was equipped in the DLS instrument and operated at a detection angle of 173°. Each 100 μL sample was prepared in a microcuvette for DLS characterization. The average self-assembled size (D_H) was recorded as a function of time at different operating temperatures (10, 15, and 25 °C). The structures of coacervates or vesicles were also observed by transmission electron microscope (TEM) (JEM 100CX-II, JEOL). The samples were incubated in a temperature-controlled digital incubator (H2200-HC, Benchmark Scientific) at different target temperatures and times, and a drop (5 μL) of each protein solution was placed on a precooled 400-mesh copper grid for 10 min at the same incubation temperature and stained with 1% phosphotungstic acid (PTA) solution for 20 s. After gentle washing with deionized water, the TEM samples were dried overnight then imaged at 100 kV.

Formation of Heterogeneous, Multi-Colored Vesicle Membranes using Different Fluorescent Fusion Proteins. Green fluorescent vesicles are formed by incubation of 1.5 μM eGFP-Z_E and 30 μM Z_R-ELP mixture solution with a NaCl concentration of 0.91 M, higher than that for mCherry vesicles, due to dimerizing preferences of eGFP head groups.[28] The T_t range of ELP fusion proteins decreases as the solution salt concentration increases (Figure S2). Therefore, the red and green fluorescent coacervates were separately formed at 10 °C at salt concentrations of 1.0 M. In all experiments, the total molar ratio of Z_E/Z_R in each protein mixture solution was 0.05 at 30 μM Z_R-ELP. To create heterogeneously multicolored vesicles, we mixed solutions of mCherry-Z_E/Z_R-ELP and eGFP-Z_E/Z_R-ELP in the coacervate phases after preaging for 30 min at 10 °C, followed by incubation postmixing for another 30 min at 10 °C to induce fusion of coacervates. Then, we increased the solution temperature of the coacervate mixture to 25 °C and characterized the vesicle membrane structures by either fluorescence microscopy (Axio Observer, Carl Zeiss) or confocal microscopy (Zeiss LSM 700, Carl Zeiss). As control groups, we also monitored vesicles made by directly heating a mixture of soluble red and green fusion proteins to 25 °C (i.e., mCherry-Z_E and eGFP-Z_E with Z_R-ELP) and red and green vesicles made separately at 25 °C and then mixed.

Mathematical Modeling to Understand the Kinetics of the Soluble-Coacervate-Vesicle Transition. A previously developed two-step nucleation model for peptide assembly[29] was modified to describe the development of vesicles transitioned from coacervates. Although two different proteins, globule-Z_E and Z_R-ELP, bound together are required for vesicles, here the model uses a single protein system for simplicity. Detailed model development is described in the SI. Briefly, the formation of coacervates is assumed to follow the classical nucleation theory that describes nucleation of droplets in vapor or solution phase.[30,31] The growth and dissolution of coacervates is assumed to be diffusion-limited,[32,33] and both depend on the free protein concentration and protein solubility. The transition from coacervate to vesicle is assumed to be a linear function of the coacervate mass. The relative concentrations of proteins in soluble form, coacervates, and vesicles were determined as a function of time. Due to the LCST behavior of ELPs, the protein solubility of the coacervate phase decreases with increasing temperature. In the simulation, the coacervate-vesicle transition happens when the temperature is greater than the midpoint of the T_t range. The midpoint is defined as the temperature presenting the highest slope change in the solution turbidity profile measured as a function of temperature. Below this temperature, the coacervate−vesicle transition rate is set to zero.

RESULTS AND DISCUSSION

Thermal Hysteresis in the Phase Transition of Globule-Z_E and Z_R-ELP Fusion Proteins. The fusion proteins, globule-Z_E and Z_R-ELP, form globule-zipper-ELP complexes in aqueous solution *via* high affinity binding of the leucine zippers and self-assemble into hollow vesicles upon warming.[25,28] We previously elucidated the correlation between the thermal driving force and the self-assembled structures with the corresponding molecular structure of the fusion proteins in terms of thermodynamic variables, protein concentration and temperature.[25] Thermodynamically, the soluble fusion proteins start to form coacervates as the

DOI: 10.1021/acs.biomac.9b00773
Biomacromolecules 2019, 20, 3494−3503

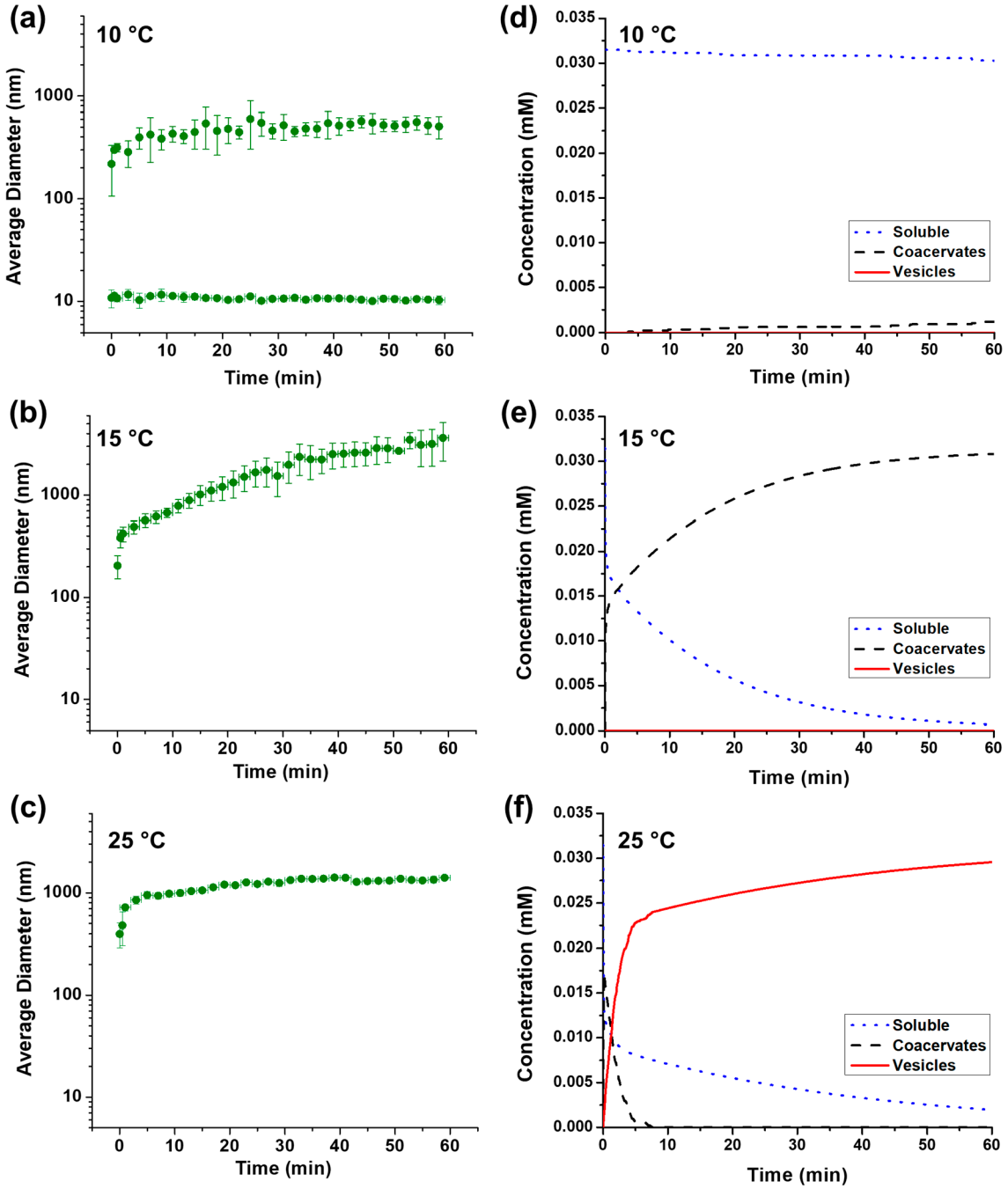

Figure 2. Changes in (a–c) average hydrodynamic diameter of fusion protein complexes (1.5 μM mCherry-Z_E and 30 μM Z_R-ELP in PBS buffer containing 0.3 M NaCl) over time at (a) 10 °C, (b) 15 °C, and (c) 25 °C, measured by dynamic light scattering (DLS). Error bars are the standard deviation of three independent measurements. (d–f) Simulation results for relative concentration profiles of soluble proteins (blue dots), coacervates (black dashes), and vesicles (red solid lines) at different temperatures ((a) 10 °C, (b) 15 °C, and (c) 25 °C).

solution temperature enters the transition range to minimize the free energy of mixing by reducing the unfavorable interactions between ELP and water as the structural transition of ELP increases its hydrophobicity.[34] Upon further heating, the amphiphilicity of the globule-zipper-ELP complexes increases due to the more collapsed hydrophobic conformation of the ELP domains, resulting in vesicle formation. Hence, the assembly of soluble ELP fusion proteins into vesicles via the coacervate phase appears to be triggered by the heat-induced phase separation of ELP.

The temperature range showing the phase transition of ELP fusion proteins is strongly dependent on amino acid composition,[35] molecular weight,[36] and environment conditions.[37,38] Thus, we first characterized the phase transition of protein complexes used in this study (1.5 μM mCherry-Z_E and 30 μM Z_R-ELP protein solution with 0.3 M NaCl) by turbidity measurements and TEM as a function of temperature (Figure 1). Protein concentration and mCherry-Z_E/Z_R-ELP molar ratio also affect the transition temperature (T_t) range, vesicle size and structure.[25,28] We chose this composition because they form single layer, micron-scale protein vesicles at room temperature. Due to the LCST behavior of ELP domains, the mixture of mCherry-Z_E and Z_R-ELP proteins are soluble at cold temperature (4 °C, phase I). An initial rapid increase in

DOI: 10.1021/acs.biomac.9b00773
Biomacromolecules 2019, 20, 3494–3503

turbidity occurs around 12 °C (phase II), followed by continued increase in turbidity and saturation of the solution turbidity profile (phase III). TEM images of samples in each phase indicate that the fusion protein complexes are soluble in phase I, undergo active inverse phase transition into coacervates in phase II, and self-assemble into stable vesicles in phase III above the midpoint of the transition phase, about 20 °C. The presence of vesicles and lack of coacervates at 20 °C (Figure 1c) indicates that vesicles form at and above the midpoint of the T_t range and do not require a temperature above the T_t range.

Figure 1b suggests that the soluble to vesicle phase transition is partially reversible with heating and cooling rates of 1 °C/min, indicating slower disassembly kinetics upon cooling. Cooling at a rate of 0.1 °C/min does not significantly change the hysteresis nor completely disassemble the vesicles (Figure S3). The complete reversibility of vesicle assembly requires >12 h at 4 °C, as confirmed in our previous work.[25] The mechanism behind the hysteresis of cooling with a slower disassembly rate is mainly thought to arise from the disruption of the PG dipeptide in ELP domains that is critical for β-turn formation.[39,40] The hysteresis in the phase transition of globule-zipper-ELP fusion proteins implies that preaging at a specific solution temperature can affect the self-assembly process and suprastructures due to the memory effect.

Kinetics of Coacervation and Vesicle Formation at Different Temperatures. To understand the kinetics of the soluble-to-coacervate and coacervate-to-vesicle transitions, we first characterized the changes in the average hydrodynamic diameter (D_H (nm)) of the self-assembled structures at different temperatures (10, 15, and 25 °C) as a function of time. As shown in Figure 2a, there are two populations observed in the protein solution at 10 °C, of which the average hydrodynamic diameters are ∼10 nm and several hundred nm. The smaller population is most likely soluble protein complexes, based on their small size. The larger population is considered to be a mixture of coacervates and aggregates, based on TEM images showing both round and irregularly shaped structures (Figure S4). However, the number density and volume density of the protein particles in DLS measurements confirm that the major population at 10 °C in phase I is soluble protein (Figure S4).

At 15 °C, only coacervates are observed by DLS and TEM and their size significantly increases over time in the microscale, indicating active growth of coacervates by either consuming soluble proteins or coalescence due to increased hydrophobicity of ELP domains (Figures 2b andS5). Even at very long time points, ranging from 1 to 7 days, only coacervates are present and vesicles are never observed, indicating that the time needed for protein reorganization is not the limiting factor in the transition from coacervates to vesicles. This demonstrates that vesicle formation requires sufficiently amphiphilic proteins with more compact, hydrophobic ELP domains that occur upon further heating above 15 °C. There may still be soluble protein in solution at 15 °C, but since DLS measurements of hydrodynamic diameter are based on the scattering intensity-weighted particle size distribution, there are technical limits to detect small soluble proteins coexisting with much larger structures that scatter significantly more light. It is not possible to separate all the coacervates formed at 15 °C by centrifugation or filtration to determine the concentration of soluble protein. However, the results of centrifugation and DLS measurements of the supernatants at 15 °C confirm that while some protein coacervates settle, those that do not can be seen to grow over time after centrifugation (Table S1, Figure S6). The growth rate of coacervates also increases with increasing incubation temperature of the protein mixture solution, as evident by comparing the slopes in Figure 2a and b. However, at 25 °C, which is above the transition range, the average diameter of the protein-assembled structures very rapidly increases within 10 min. The rate of size increase gradually declines over time and stabilizes within 1 h (Figure 2c). The changes in solution turbidity over time also correspond to the size changes of supra-structures in the mCherry-Z_E and Z_R-ELP mixture solution (Figure S7).

Coacervate and vesicle formation are simulated with a protein assembly model under a two-step nucleation mechanism.[29−31] Additional details on model development are provided in the SI. For simplicity, the two-component system with mCherry-Z_E and Z_R-ELP is reduced to a single component system in the simulation, which uses the properties of Z_R-ELP for the parameters, including the molecular weight, protein concentration, and protein density. The rest of the parameters are selected to match nucleus size and nucleation rate for coacervates from the experimental results (Tables S2 and S3). Using a Monte Carlo algorithm,[41] the model follows the overall protein distribution between the free protein, coacervate, and vesicle phases (Figure 2d−f).

This model provides an explanation for the experimental results. The light scattering measurement at 10 °C (Figures 2a and S4a-b) suggests that most of the proteins remain soluble. The majority of the solution is composed of free soluble proteins and little protein participates in coacervate assembly at this temperature (Figure 2d), thus the size of coacervates does not increase remarkably after their nucleation. The parameter set for the model is designed to reproduce these system behaviors and tuned for the experimental data obtained at three different temperatures of 10 °C, 15 °C, and 25 °C. The kinetic parameters, Flory−Huggins parameter (χ), rate constant for coacervate growth (k_{g1}), and vesicle nucleation constant (k_n) are summarized in Table S2 in the SI. Increasing the temperature to 15 °C decreases the protein solubility, increasing coacervate growth. This is apparent by the significant increase in the number of proteins assembled into coacervates while consuming free soluble proteins (Figure 2e), which corresponds to the DLS experimental results (Figure 2b). The simulation suggests that the temperature change strongly affects the kinetic properties of either coacervation growth or vesicle formation rates, accompanied by the changes in ELP solubility that acts as a driving force on the coacervate to vesicle transition. Finally, vesicles formed almost instantly at 25 °C, which is above T_t range, and the average vesicle size increased slowly with time (Figure 2f). The modeling results suggested that the thermodynamic and kinetic properties of the coacervate-to-vesicle transition system significantly depend on the temperature. Therefore, we performed the following experiments under constant temperature or with a step temperature change for consistent analysis.

To trace the structural changes of suprastructures made from mCherry-Z_E and Z_R-ELP upon warming from 4 to 25 °C, we monitored *in situ* fluorescent images from a solution containing the fusion protein complexes and prepared corresponding TEM samples (Figure 3). A movie showing the fluorescent *in situ* monitoring of morphological changes in the self-assembled structures in the protein mixture solution is available in the SI. Instant nucleation of coacervates was

DOI: 10.1021/acs.biomac.9b00773
Biomacromolecules 2019, 20, 3494−3503

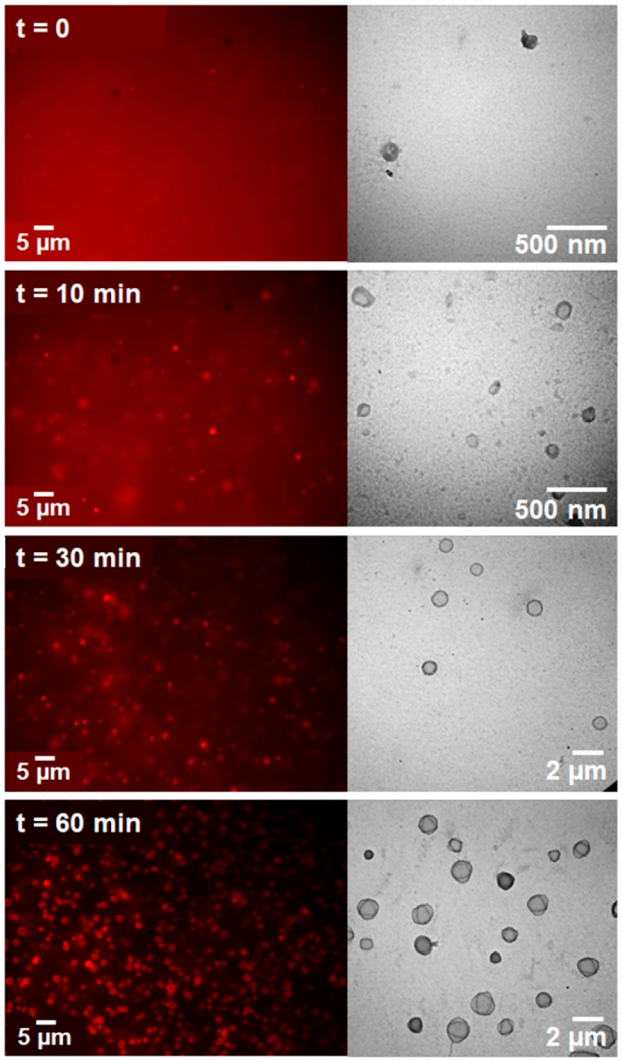

Figure 3. Fluorescent micrographs (left) and transmission electron micrographs (right) of the self-assembled structures in a protein solution of mCherry-Z_E and Z_R-ELP mixtures starting at 4 °C and warmed to room temperature (~25 °C) at different times (right after, 10 min, 30, and 60 min).

observed at the beginning, but they rapidly transitioned into small vesicles within 10 min upon warming, as confirmed by TEM images. The fluorescence intensity of the surrounding solution decreased over time, while the fluorescence intensity of structures increased. This implies that small vesicles, which quickly transitioned from the nucleated small coacervates while passing through the T_t range during warming from 4 to 25 °C, can grow by consuming remaining soluble proteins. Vesicle formation at 25 °C is stable within 1 h.

The observation of size and structural changes of mCherry-Z_E and Z_R-ELP fusion protein mixtures along with the simulation results demonstrate that the proteins present different rates of coacervation and vesicle formation as a function of temperature. Also, the growth rates of coacervates and vesicles are dictated by the relative concentration between free soluble proteins and proteins in coacervates or vesicles. These results also indicate that temperature and time can be critical to controlling the self-assembled protein structures. Therefore, we investigated the effects of preaging the protein mixture solutions at different temperatures (at 10 and 15 °C in phase I and II, respectively) on the vesicle structures, which are formed by additional warming to 25 °C.

Effect of Aging the Fusion Protein Solution at Different Temperatures on the Transitioned Vesicle Properties. The fusion protein amphiphiles, which form coacervate droplets with hydrophobically collapsed ELP domains, rearrange and transform themselves into hollow vesicles upon further heating above the midpoint of the T_t range. In the mathematical models to support the coacervate-to-vesicle transition, we assumed that the coacervates directly become vesicles. To confirm the effect of initial structural properties of coacervates on the structure of the transitioned vesicles, we preaged protein solutions in the coacervate phase separately for different times (10, 30, and 60 min) at the sub-T_t range and low-T_t range temperatures of 10 and 15 °C, respectively, and triggered vesicle transition by further warming the solutions to 25 °C in series.

We characterized the size and morphology of the vesicles transitioned from the preaged coacervates (Figure 4). The structural properties of protein vesicles formed at 25 °C after preaging at 10 °C have no significant differences in terms of vesicle size compared to the standard vesicle formed by direct warming to 25 °C (Figures S8 and S9). This is expected because the majority of proteins remain soluble at 10 °C, as confirmed in Figures 2a and S4. Alternatively, preaging protein solutions in the coacervate growth phase at 15 °C shows a significant increase in the vesicle size. The increase in size of coacervate droplets over 60 min implies that more proteins assemble into coacervate droplets by consuming soluble proteins and/or coalescence of coacervates with time. Interestingly, we confirmed that the average sizes of preaged coacervates and transitioned vesicles before and after the heat trigger are similar (Figures S8 and S10). This result can support our modeling hypothesis that all proteins assembled in a coacervate are involved in the transition to form a vesicle. An instant increase in coacervate size was followed by rapid decrease and stabilization in size upon the 25 °C heat trigger for vesicle transition suggests that there is an expansion of coacervate droplets and rearrangement of the protein amphiphiles into vesicles (Figure S8). Vesicles transitioned from coacervates preaged at 15 °C for 1 h displayed a diameter of about 4 μm, which is over twice the diameter of vesicles directly assembled from soluble proteins.

As a result, we confirmed the size of coacervated assemblies before the vesicle transition is critical to dictate the size of vesicles. The relative concentration of proteins found in the solution and in the coacervate droplets dictates the vesicle formation kinetics, and bigger coacervates lead to formation of bigger vesicles. In our previous studies,[25,28] we demonstrated that the size of protein vesicles can be controlled in a range from a few hundred nm to 2 μm, by tuning either the molar ratio of mCherry-Z_E to Z_R-ELP or the total protein concentration, which are all discontinuous variables that require different sample preparation. Here, by simply changing the temperature and preaging time in a solution, we were able to expand the range of the vesicle size up to 4 μm, which can be used as microreactors or for encapsulation of nano- or micron-sized objects. Also, temperature and time are independent but continuous variables. We only applied stepwise triggers of temperature and time for the protein phase transition in this study to clearly demonstrate the effect of preaged coacervates on the transitioned vesicles. The effect

DOI: 10.1021/acs.biomac.9b00773
Biomacromolecules 2019, 20, 3494−3503

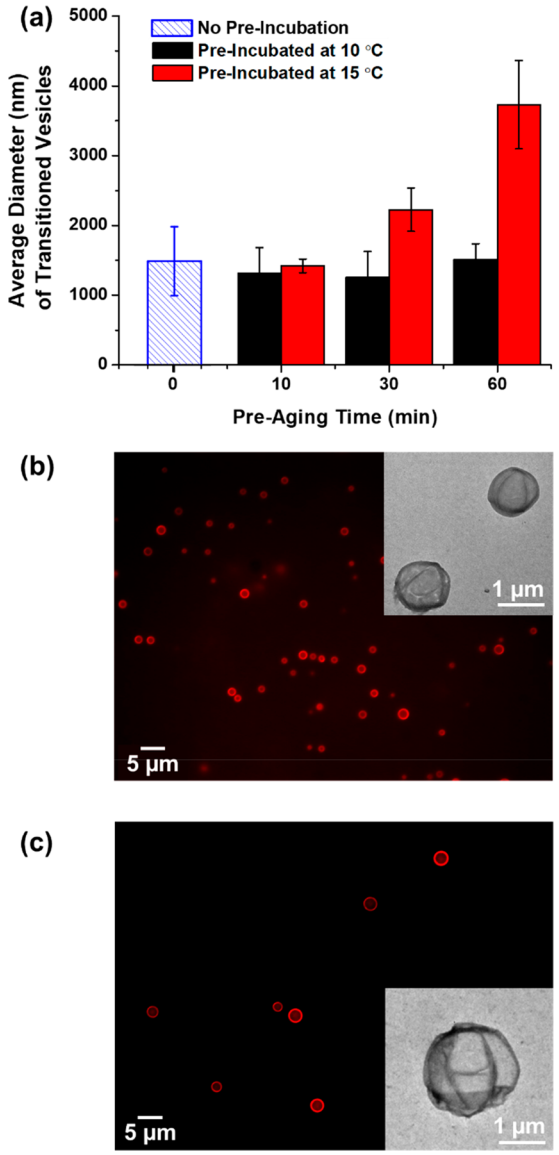

Figure 4. (a) Average diameter of the vesicles transitioned from coacervates preaged at 10 °C (black) and 15 °C (red) for different times (10, 30, and 60 min). The bar filled with blue lines represents the average diameter of the control vesicles directly incubated at 25 °C from soluble proteins without preaging. (b, c) Fluorescent and TEM (inset) images of the transitioned vesicles after preaging at (b) 10 °C and (c) 15 °C for 60 min.

of heating rate on the vesicle formation and vesicle properties will warrant more detailed investigation in future work.

Engineering Membrane Structure of Globular Protein Vesicles by Tuning Coacervate Phase. The similar average sizes between preaged coacervates and transitioned vesicles before and after the 25 °C heat trigger, as shown in Figure S10, raised the question of whether the vesicle membrane composition could be tuned via engineering the coacervate phase. As a proof of concept, we used two different types of globular proteins, mCherry-Z_E and eGFP-Z_E, which make red and green fluorescent vesicles, respectively.[28] We previously confirmed that vesicle self-assembly of globule-Z_E/Z_R-ELP protein mixtures was only achieved above a critical salt concentration depending on the globular domain type, namely 0.30 M for mCherry and 0.91 M for eGFP.[28] This is hypothesized to be due to the dimerizing nature of eGFP. Since the ELP transition is also strongly dependent on salt concentration, we first characterized the transition temperature range of eGFP-Z_E/Z_R-ELP complexes at 1.0 M salt concentration (Figure S2a). Similarly, we investigated the effect of salt concentration on the midtransition temperature range of mCherry-Z_E and Z_R-ELP mixtures (Figure S2b). This information enabled selection of mixing temperatures at which both mCherry and eGFP complexes are either coacervates or vesicles. On the basis of the results, red (mCherry) and green (eGFP) soluble, coacervate, and vesicle phases were mixed together at 4 °C, 10 °C, and 25 °C, respectively, at 1.0 M salt concentration.

In general, protein mobility decreases within dense coacervate droplets with higher viscosity than free solutions.[42] Therefore, we hypothesized that the fusion of red and green coacervates with limited diffusion of each protein building block, followed by a rapid transition into vesicles, would be able to create different membrane domains in vesicles. To address this question, we monitored the membrane composition of red and green vesicles prepared by three different incubation pathways: (Path 1) vesicles directly transitioned from soluble red and green protein mixtures, (Path 2) vesicles transitioned from mixtures of separately preincubated red and green coacervates, and (Path 3) separate red and green vesicles mixed after transition (Figure 5).

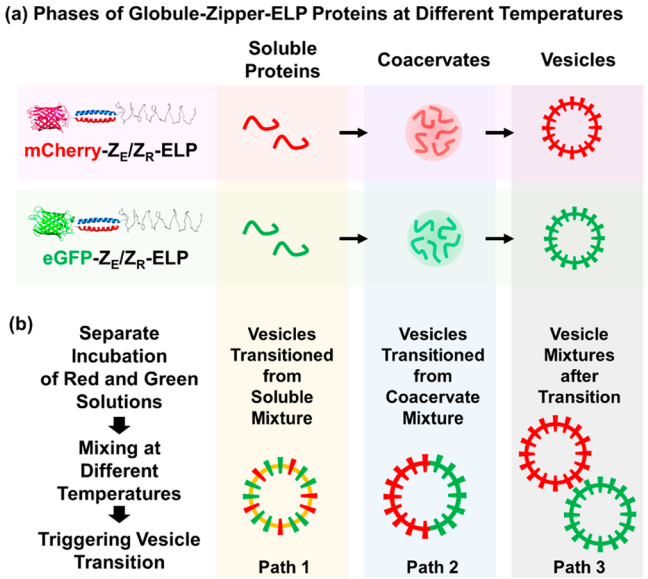

Figure 5. A schematic illustration of experimental groups to trace coacervate-to-vesicle transition. (a) Soluble proteins of either mCherry-Z_E/Z_R-ELP or eGFP-Z_E/Z_R-ELP fusion protein complexes transition into red or green fluorescent vesicles through coacervates with increasing temperature. (b) We prepared three different groups of vesicle samples controlled by different incubation pathways: (Path 1) vesicles directly transitioned from soluble protein mixtures, (Path 2) vesicles transitioned from mixtures of coacervates, and (Path 3) vesicles mixed after transition from coacervates.

The soluble protein mixtures of red fluorescent mCherry-Z_E/Z_R-ELP and green fluorescent eGFP-Z_E/Z_R-ELP resulted in homogeneous "yellow" protein vesicle membranes (Figure 6a), which means the two different fluorescent building blocks randomly and homogeneously coacervate and transition into vesicles upon warming to 25 °C, as previously confirmed.[28]

DOI: 10.1021/acs.biomac.9b00773
Biomacromolecules 2019, 20, 3494−3503

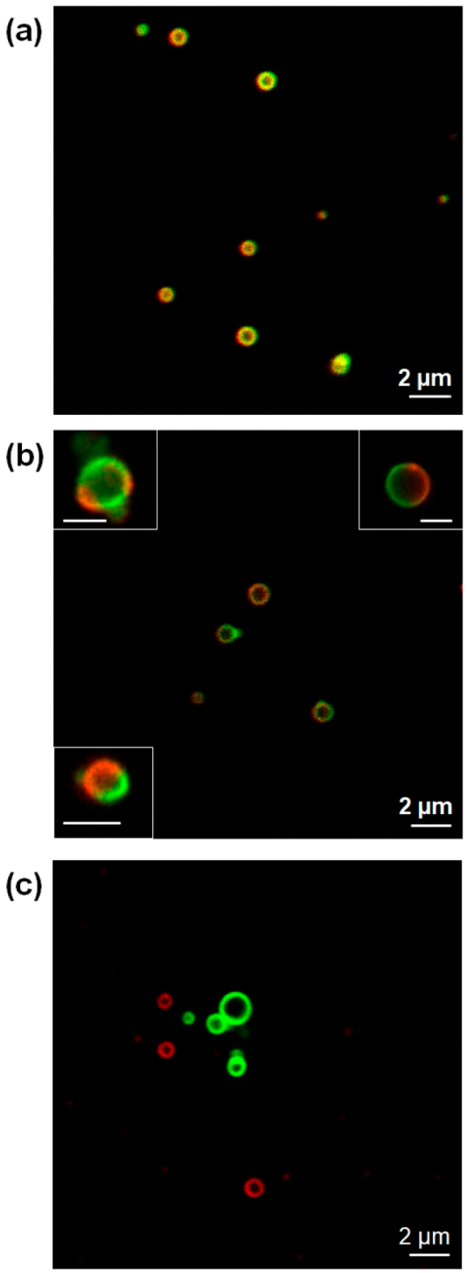

Figure 6. Engineering vesicle membrane composition by tuning solution incubation pathways: (a) homogeneous red and green protein "yellow" vesicles made from soluble protein mixtures, (b) partially segregated, heterogeneous protein vesicles transitioned from red and green coacervate mixtures, and (c) single color red and green vesicles mixed after transition.

However, when red and green coacervate solutions were made separately and then mixed together, warming to 25 °C produced vesicles with red and green partially segregated and multicolored membranes (Figure 6b). Confocal images (Figure S11) demonstrated that the segregation is randomly distributed in vesicle membrane, as expected since coacervate collision and fusion should be random. In this case, we separately preaged the red and green protein coacervate solutions for 30 min, mixed the solutions, and incubated the coacervate mixture 30 min more to induce fusion of the red and green coacervates. Then, we warmed the mixed solution to room temperature to trigger the coacervate-to-vesicle transition. The coacervate mixtures cannot be fully mixed in 30 min due to the limited mobility at the interface, which leads to the formation of heterogeneous membrane organization after the temperature-induced vesicle transition. We analyzed the percentage of heterogeneous vesicles and determined that about 16% of vesicles are heterogeneous when made from coacervate mixtures incubated together for 30 min. 100% of vesicles are homogeneous (yellow) when formed from soluble protein mixtures and 100% of vesicles are homogeneous (either red or green) when red and green vesicles are mixed. Aging longer than 30 min after mixing the red and green coacervates at low transition temperatures resulted in more homogeneous vesicle membranes similar to soluble mixtures, whereas shorter mixing time induced more distinct vesicle membrane domains (Figure S12). Finally, no fusion events happened in the mixed solutions of red and green vesicles separately transitioned from red and green coacervates (Figure 6c).

When the vesicle membrane presents a heterogeneous morphology, it may have more complex and sophisticated functionalities than vesicles with a homogeneous structure.[43,44] To date, phase separation of mixed membranes composed of lipid mixtures has been actively studied and used to produce membrane heterogeneity in vesicles.[45,46] To our knowledge, this is the first report to show heterogeneous vesicle membranes composed of two different kinds of globular protein domains. In addition, protein vesicles with membrane heterogeneity were created by the simple self-assembly process tuned by temperature and time in a mild aqueous environment without hampering bioactivity of the incorporated globular proteins. We observed that the segregated domains become homogeneous approximately 4 h after formation (Figure S13). This indicates that the vesicle membrane is fluid and protein diffusion can occur. More precise control over the membrane heterogeneity and fluidity with a thorough understanding of phase separation of two different kinds of fusion protein building blocks is necessary to achieve potential applications of heterogeneous protein vesicles.

CONCLUSIONS

To find a rational strategy for engineering the size and heterogeneity of protein vesicles self-assembled from globule-Z_E and Z_R-ELP fusion proteins, we focused on understanding the phase transition kinetics from soluble proteins to vesicles through the coacervate phase. First, we demonstrated that the soluble protein-to-coacervate transition accelerates when the temperature enters the transition range, and the coacervates continue to grow as a function of aging time at temperatures below the midpoint of the transition range. The growth rate of coacervates also increased as the solution temperature increased. In addition, we confirmed that the size and composition of coacervates dictate the size and membrane organization of the transitioned vesicles formed upon further heating. Therefore, controlling the solution temperature and preaging time in the coacervate phase resulted in different sized transitioned vesicles, from 1 to 4 μm. On the basis of the experimental observations and mathematical modeling to support the transition kinetics, we were able to create heterogeneous protein vesicles by inducing fusion in the coacervate phase. The mathematical model discussed in this study can also be generally applicable to a wide range of proteins that form high-order assembled structures from pre-existing coacervates. The present study gives fundamental and

DOI: 10.1021/acs.biomac.9b00773
Biomacromolecules 2019, 20, 3494−3503

practical insights into understanding how protein coacervates grow and assemble into organized structures.

■ ASSOCIATED CONTENT

Supporting Information

The Supporting Information is available free of charge on the ACS Publications website at DOI: 10.1021/acs.biomac.9b00773.

Figures S1−S13, Tables S1−S3, Mathematical Model Development (PDF)

Fluorescent in situ monitoring of morphological changes in the self-assembled structures (AVI)

■ AUTHOR INFORMATION

Corresponding Author

*E-mail: julie.champion@chbe.gatech.edu.

ORCID

Martha A. Grover: 0000-0002-7036-776X

Julie A. Champion: 0000-0002-0260-9392

Present Address

‖(Y.J.) Department of Chemical Engineering, University of Florida, 1030 Center Drive, Gainesville, Florida 32611, United States.

Author Contributions

The manuscript was written through contributions of all authors. All authors have given approval to the final version of the manuscript.

Funding

This research was financially supported by the National Science Foundation Division of Materials Research, Award Number 1709428. This work was performed in part at the Georgia Tech Institute for Electronics and Nanotechnology, a member of the National Nanotechnology Coordinated Infrastructure, which is supported by the National Science Foundation (Grant No. ECCS-1542174). This work was supported in part by Dr. Jang's startup funds provided by the Department of Chemical Engineering at the University of Florida. We wish to acknowledge the core facilities at the Parker H. Petit Institute for Bioengineering and Bioscience at the Georgia Institute of Technology and BME (J. Crayton Pruitt Family Department of Biomedical Engineering) Core Facility, Herbert Wertheim College of Engineering at the University of Florida for the use of their shared equipment, services, and expertise. Some of this work was performed in part at the Georgia Tech Institute for Electronics and Nanotechnology, a member of the National Nanotechnology Coordinated Infrastructure, which is supported by the National Science Foundation (Grant No. ECCS-1542174).

Notes

The authors declare no competing financial interest.

■ ACKNOWLEDGMENTS

The authors acknowledge Prof. D. Tirrell and Prof. K. Zhang for DNA plasmids. We also acknowledge Clark Vu for assistance with protein expression, purification, and preparation of vesicle samples.

■ REFERENCES

(1) van Niel, G.; D'Angelo, G.; Raposo, G. Shedding light on the cell biology of extracellular vesicles. *Nat. Rev. Mol. Cell Biol.* **2018**, *19*, 213.

(2) Discher, D. E.; Ahmed, F. POLYMERSOMES. *Annu. Rev. Biomed. Eng.* **2006**, *8* (1), 323−341.

(3) Rideau, E.; Dimova, R.; Schwille, P.; Wurm, F. R.; Landfester, K. Liposomes and polymersomes: a comparative review towards cell mimicking. *Chem. Soc. Rev.* **2018**, *47* (23), 8572−8610.

(4) Kauscher, U.; Holme, M. N.; Björnmalm, M.; Stevens, M. M. Physical stimuli-responsive vesicles in drug delivery: Beyond liposomes and polymersomes. *Adv. Drug Delivery Rev.* **2019**, *138*, 259−275.

(5) Ki, S. H.; Park, J. K.; Sung, C.; Lee, C. B.; Uhm, H.; Choi, E. H.; Baik, K. Y. Artificial vesicles as an animal cell model for the study of biological application of non-thermal plasma. *J. Phys. D: Appl. Phys.* **2016**, *49* (8), 085401.

(6) Elani, Y.; Trantidou, T.; Wylie, D.; Dekker, L.; Polizzi, K.; Law, R. V.; Ces, O. Constructing vesicle-based artificial cells with embedded living cells as organelle-like modules. *Sci. Rep.* **2018**, *8* (1), 4564.

(7) Wang, L.; Wen, P.; Liu, X. M.; Zhou, Y. T.; Li, M.; Huang, Y. D.; Geng, L.; Mann, S.; Huang, X. Single-step fabrication of multicompartmentalized biphasic proteinosomes. *Chem. Commun.* **2017**, *53* (61), 8537−8540.

(8) Elani, Y.; Law, R. V.; Ces, O. Vesicle-based artificial cells as chemical microreactors with spatially segregated reaction pathways. *Nat. Commun.* **2014**, *5*, 5305.

(9) Arriaga, L. R.; Huang, Y.; Kim, S.-H.; Aragones, J. L.; Ziblat, R.; Koehler, S. A.; Weitz, D. A. Single-step assembly of asymmetric vesicles. *Lab Chip* **2019**, *19* (5), 749−756.

(10) Weiss, M.; Frohnmayer, J. P.; Benk, L. T.; Haller, B.; Janiesch, J. W.; Heitkamp, T.; Borsch, M.; Lira, R. B.; Dimova, R.; Lipowsky, R.; et al. Sequential bottom-up assembly of mechanically stabilized synthetic cells by microfluidics. *Nat. Mater.* **2018**, *17* (1), 89.

(11) Wang, M.; Liu, Z.; Zhan, W. Janus Liposomes: Gel-Assisted Formation and Bioaffinity-Directed Clustering. *Langmuir* **2018**, *34* (25), 7509−7518.

(12) Weinberger, A.; Tsai, F.-C.; Koenderink, G. H.; Schmidt, T. F.; Itri, R.; Meier, W.; Schmatko, T.; Schroder, A.; Marques, C. Gel-Assisted Formation of Giant Unilamellar Vesicles. *Biophys. J.* **2013**, *105* (1), 154−164.

(13) Vieregg, J. R.; Tang, T. Y. D. Polynucleotides in cellular mimics: Coacervates and lipid vesicles. *Curr. Opin. Colloid Interface Sci.* **2016**, *26*, 50−57.

(14) Hyman, A. A.; Weber, C. A.; Juelicher, F. Liquid-Liquid Phase Separation in Biology. *Annu. Rev. Cell Dev. Biol.* **2014**, *30*, 39−58.

(15) Yeo, G. C.; Keeley, F. W.; Weiss, A. S. Coacervation of tropoelastin. *Adv. Colloid Interface Sci.* **2011**, *167* (1−2), 94−103.

(16) McDaniel, J. R.; Callahan, D. J.; Chilkoti, A. Drug delivery to solid tumors by elastin-like polypeptides. *Adv. Drug Delivery Rev.* **2010**, *62* (15), 1456−1467.

(17) Betre, H.; Ong, S. R.; Guilak, F.; Chilkoti, A.; Fermor, B.; Setton, L. A. Chondrocytic differentiation of human adipose-derived adult stem cells in elastin-like polypeptide. *Biomaterials* **2006**, *27* (1), 91−99.

(18) Simon, J. R.; Carroll, N. J.; Rubinstein, M.; Chilkoti, A.; Lopez, G. P. Programming molecular self-assembly of intrinsically disordered proteins containing sequences of low complexity. *Nat. Chem.* **2017**, *9* (6), 509−515.

(19) Blocher, W. C.; Perry, S. L. Complex coacervate-based materials for biomedicine. *Wiley Interdisciplinary Reviews: Nanomedicine and Nanobiotechnology* **2017**, *9* (4), No. e1442.

(20) Imura, T.; Yanagishita, H.; Kitamoto, D. Coacervate formation from natural glycolipid: One acetyl group on the headgroup triggers coacervate-to-vesicle transition. *J. Am. Chem. Soc.* **2004**, *126* (35), 10804−10805.

(21) Oana, H.; Kishimura, A.; Yonehara, K.; Yamasaki, Y.; Washizu, M.; Kataoka, K. Spontaneous Formation of Giant Unilamellar Vesicles from Microdroplets of a Polyion Complex by Thermally Induced Phase Separation. *Angew. Chem., Int. Ed.* **2009**, *48* (25), 4613−4616.

(22) Ianiro, A.; Wu, H. L.; van Rijt, M. M. J.; Vena, M. P.; Keizer, A. D. A.; Esteves, A. C. C.; Tuinier, R.; Friedrich, H.; Sommerdijk, N. A.

DOI: 10.1021/acs.biomac.9b00773
Biomacromolecules 2019, 20, 3494−3503

J. M.; Patterson, J. P. Liquid-liquid phase separation during amphiphilic self-assembly. *Nat. Chem.* **2019**, *11* (4), 320−328.
(23) Flory, P. J. Thermodynamics of Dilute Solutions of High Polymers. *J. Chem. Phys.* **1945**, *13* (11), 453−465.
(24) Sato, T.; Takahashi, R. Competition between the micellization and the liquid−liquid phase separation in amphiphilic block copolymer solutions. *Polym. J.* **2017**, *49*, 273.
(25) Jang, Y.; Choi, W. T.; Heller, W. T.; Ke, Z. L.; Wright, E. R.; Champion, J. A., Engineering Globular Protein Vesicles through Tunable Self-Assembly of Recombinant Fusion Proteins. *Small* **2017**,*13*, 1700399.
(26) Park, W. M.; Champion, J. A. Two-Step Protein Self-Assembly in the Extracellular Matrix. *Angew. Chem., Int. Ed.* **2013**, *52* (31), 8098−8101.
(27) Moll, J. R.; Ruvinov, S. B.; Pastan, I.; Vinson, C. Designed heterodimerizing leucine zippers with a range of pIs and stabilities up to 10(−15) M. *Protein Sci.* **2001**, *10* (3), 649−655.
(28) Park, W. M.; Champion, J. A. Thermally Triggered Self-Assembly of Folded Proteins into Vesicles. *J. Am. Chem. Soc.* **2014**, *136* (52), 17906−17909.
(29) Hsieh, M.-C.; Lynn, D. G.; Grover, M. A. A Kinetic Model for Two-Step Nucleation of Peptide Assembly. *J. Phys. Chem. B* **2017**, *121*, 7401.
(30) Erdemir, D.; Lee, A. Y.; Myerson, A. S. Nucleation of Crystals from Solution: Classical and Two-Step Models. *Acc. Chem. Res.* **2009**, *42* (5), 621−629.
(31) Tauer, K.; Kuhn, I. Modeling Particle Formation in Emulsion Polymerization - an Approach by Means of the Classical Nucleation Theory. *Macromolecules* **1995**, *28* (7), 2236−2239.
(32) Vetter, T.; Iggland, M.; Ochsenbein, D. R.; Hanseler, F. S.; Mazzotti, M. Modeling Nucleation, Growth, and Ostwald Ripening in Crystallization Processes: A Comparison between Population Balance and Kinetic Rate Equation. *Cryst. Growth Des.* **2013**, *13* (11), 4890−4905.
(33) Matthews, H. B.; Miller, S. M.; Rawlings, J. B. Model identification for crystallization: Theory and experimental verification. *Powder Technol.* **1996**, *88* (3), 227−235.
(34) Li, N. K.; Quiroz, F. G.; Hall, C. K.; Chilkoti, A.; Yingling, Y. G. Molecular Description of the LCST Behavior of an Elastin-Like Polypeptide. *Biomacromolecules* **2014**, *15* (10), 3522−3530.
(35) Christensen, T.; Hassouneh, W.; Trabbic-Carlson, K.; Chilkoti, A. Predicting Transition Temperatures of Elastin-Like Polypeptide Fusion Proteins. *Biomacromolecules* **2013**, *14* (5), 1514−1519.
(36) Teeuwen, R. L. M.; de Wolf, F. A.; Zuilhof, H.; van Hest, J. C. M. Elastin-like polypeptides of different molecular weights show independent transition temperatures when mixed. *Soft Matter* **2009**, *5* (21), 4305−4310.
(37) MacKay, J. A.; Callahan, D. J.; FitzGerald, K. N.; Chilkoti, A. Quantitative Model of the Phase Behavior of Recombinant pH-Responsive Elastin-Like Polypeptides. *Biomacromolecules* **2010**, *11* (11), 2873−2879.
(38) Cho, Y.; Zhang, Y.; Christensen, T.; Sagle, L. B.; Chilkoti, A.; Cremer, P. S. Effects of Hofmeister Anions on the Phase Transition Temperature of Elastin-like Polypeptides. *J. Phys. Chem. B* **2008**, *112* (44), 13765−13771.
(39) Lyons, D. F.; Le, V.; Bidwell, G. L.; Kramer, W. H.; Lewis, E. A.; Raucher, D.; Correia, J. J. Structural and Hydrodynamic Analysis of a Novel Drug Delivery Vector: ELP[V(5)G(3)A(2)-150]. *Biophys. J.* **2013**, *104* (9), 2009−2021.
(40) Reguera, J.; Lagaron, J. M.; Alonso, M.; Reboto, V.; Calvo, B.; Rodriguez-Cabello, J. C. Thermal behavior and kinetic analysis of the chain unfolding and refolding and of the concomitant nonpolar solvation and desolvation of two elastin-like polymers. *Macromolecules* **2003**, *36* (22), 8470−8476.
(41) Wang, L.; Broadbelt, L. J. Tracking Explicit Chain Sequence in Kinetic Monte Carlo Simulations. *Macromol. Theory Simul.* **2011**, *20* (1), 54−64.
(42) Kayitmazer, A. B.; Bohidar, H. B.; Mattison, K. W.; Bose, A.; Sarkar, J.; Hashidzume, A.; Russo, P. S.; Jaeger, W.; Dubin, P. L. Mesophase separation and probe dynamics in protein-polyelectrolyte coacervates. *Soft Matter* **2007**, *3* (8), 1064−1076.
(43) Beales, P. A.; Nam, J.; Vanderlick, T. K. Specific adhesion between DNA-functionalized "Janus" vesicles: size-limited clusters. *Soft Matter* **2011**, *7* (5), 1747−1755.
(44) Liu, Y. J.; Yang, X. Y.; Huang, Z. Q.; Huang, P.; Zhang, Y.; Deng, L.; Wang, Z. T.; Zhou, Z. J.; Liu, Y.; Kalish, H.; Khachab, N. M.; Chen, X. Y.; Nie, Z. H. Magneto-Plasmonic Janus Vesicles for Magnetic Field-Enhanced Photoacoustic and Magnetic Resonance Imaging of Tumors. *Angew. Chem., Int. Ed.* **2016**, *55* (49), 15297−15300.
(45) Semrau, S.; Schmidt, T. Membrane heterogeneity - from lipid domains to curvature effects. *Soft Matter* **2009**, *5* (17), 3174−3186.
(46) Veatch, S. L.; Keller, S. L. Separation of liquid phases in giant vesicles of ternary mixtures of phospholipids and cholesterol. *Biophys. J.* **2003**, *85* (5), 3074−3083.

DOI: 10.1021/acs.biomac.9b00773
Biomacromolecules 2019, 20, 3494−3503